Journal of Power Sources 109 (2002) 253–261
JOURNAL OF POWER SOURCES
www.elsevier.com/locate/jpowsour

An Op Amp transfer circuit to measure voltages in battery strings

X. Wang, T. Stuart*
University of Toledo, Toledo, OH, USA

Received 6 November 2001; accepted 14 January 2002

Abstract

To measure the individual voltages in a series connected battery pack, each measurement must be transferred to a common reference level. A transconductance amplifier using an operational amplifier (Op Amp) provides a convenient circuit that is both simple and cost effective. This technique is shown to be more accurate than previous methods and it avoids most of the component matching requirements

Keywords: Lithium ion batteries; Lead-acid batteries; Nickel metal hybrid batteries; Voltage measurement

1. Introduction

Applications such as electric vehicles and uninterruptable power supplies require the use of large packs of series connected batteries (battery strings). Some of these applications require monitoring equipment that is capable of measuring the voltages of individual battery segments within the pack in order to prevent damage and identify defective segments. As discussed in [1–3,13], most types of batteries can be damaged by excessively high or low voltages and in some cases the results can be catastrophic. Lithium ion cells, for example, will ignite if their voltages become too high, which equates to an over-charged condition. Therefore, once high or low voltage segments have been identified, some equalization process must be used to re-balance the voltages [4–12]. Imbalances are especially prevalent in applications, such as electric vehicles where the batteries are frequently charged and discharged. Certain problems associated with these measurements also were previously described in [13], along with possible solutions.

To process the data at a central location, these measurement circuits must transfer each segment voltage to a common reference level, such as the system ground as shown in Fig. 1. Fig. 2 shows the block diagram of a typical modularized battery management system that would use one of these transfer circuits in each of the local modules, LM nos.1–4. In this system the four local modules are used to obtain data from four sections of a series battery pack, where each section contains 12 segments that require voltage measurements. One advantage of this type of system is that only a few of wires are required to transfer power and data between the local and central modules (CM). This particular system uses four wires: two for powering the LMs and two for the differential serial data bus. This modularized approach drastically reduces the amount of wiring that otherwise would be required between the CM and the batteries. The transfer circuit in each LM is used to shift all 12 measurements to its local ground references, i.e. G1–G4. These voltages are then multiplexed, fed to an A/D converter, processed by a local microcontroller and galvanically transmitted to the CM via a serial bus, such as CAN 2.0B.

Reference [13] also proposed a transfer circuit using discrete transistors for performing these measurements. An example of this circuit is shown in Fig. 3. This system provides several accuracy and cost advantages over previous methods and it also can be used for any number of battery segments, i.e., Bl to Bn in Fig. 1. This is an important advantage for these modular measurement systems because each LM can measure a large number of segments to reduce the number of LMs. For a 48-cell pack, for example, 4 LMs each measuring 12 cells can be used in place of perhaps 12 LMs each measuring 4 cells. This represents a large cost savings since, as shown in Fig. 2, each LM typically contains a multiplexer, A/D converter, microcontroller and two galvanically isolated buffers for the serial data bus. Although effective, this earlier transfer circuit does depend on matching discrete components to reduce errors caused by temperature changes. This is of special importance for automotive applications where the operating range for the electronics may approach −30 to + 50 °C, even though the useful range for the battery itself is more narrow [3].

* Corresponding author. Tel.: +1-419-530-8140; fax: +1-419-530-8146.
E-mail address: tstuart@uofto2.toledo.edu (T. Stuart).

0378-7753/02/$ – see front matter © 2002 Published by Elsevier Science B.V.
PII: S0378-7753(02)00042-3

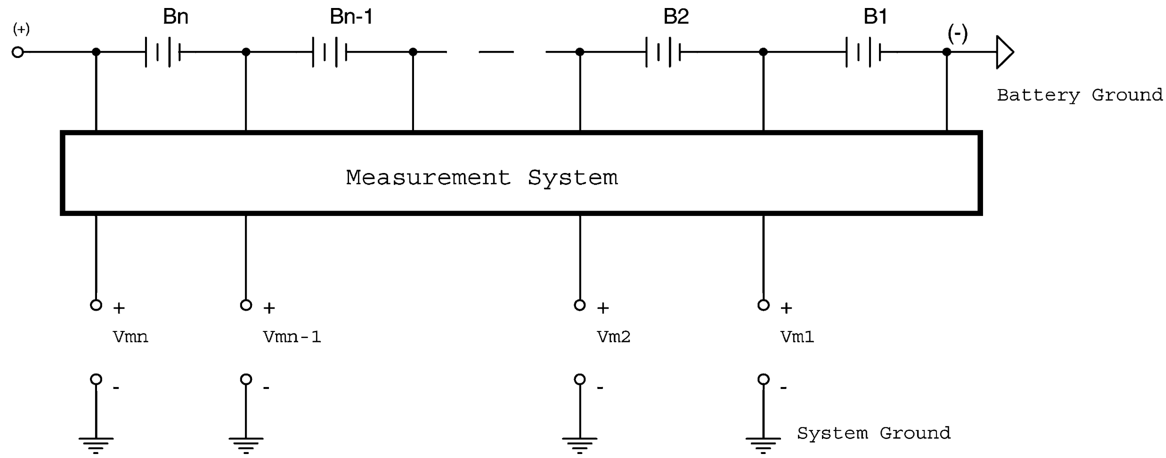

Fig. 1. Voltage measurement system for a series battery pack.

Continuing research has produced an alternative circuit, shown in Fig. 4, that simplifies the component matching requirements by using an operational amplifier (Op Amp) in place of discrete transistors. This circuit has already proven to be effective for lower voltage segments below 5 V dc, which is satisfactory for applications, such as lithium ion (Li-ion) batteries which are typically <4 V dc. However, care must be taken to avoid certain leakage current paths that exist while the circuit is supposed to be inactive. The identification of these paths and methods for eliminating them will be described along with experimental results.

2. Previous research

Reference [13] proposed the transfer circuit in Fig. 3 to perform the required voltage shifting for measuring the segment voltages in a series battery pack. As stated earlier,

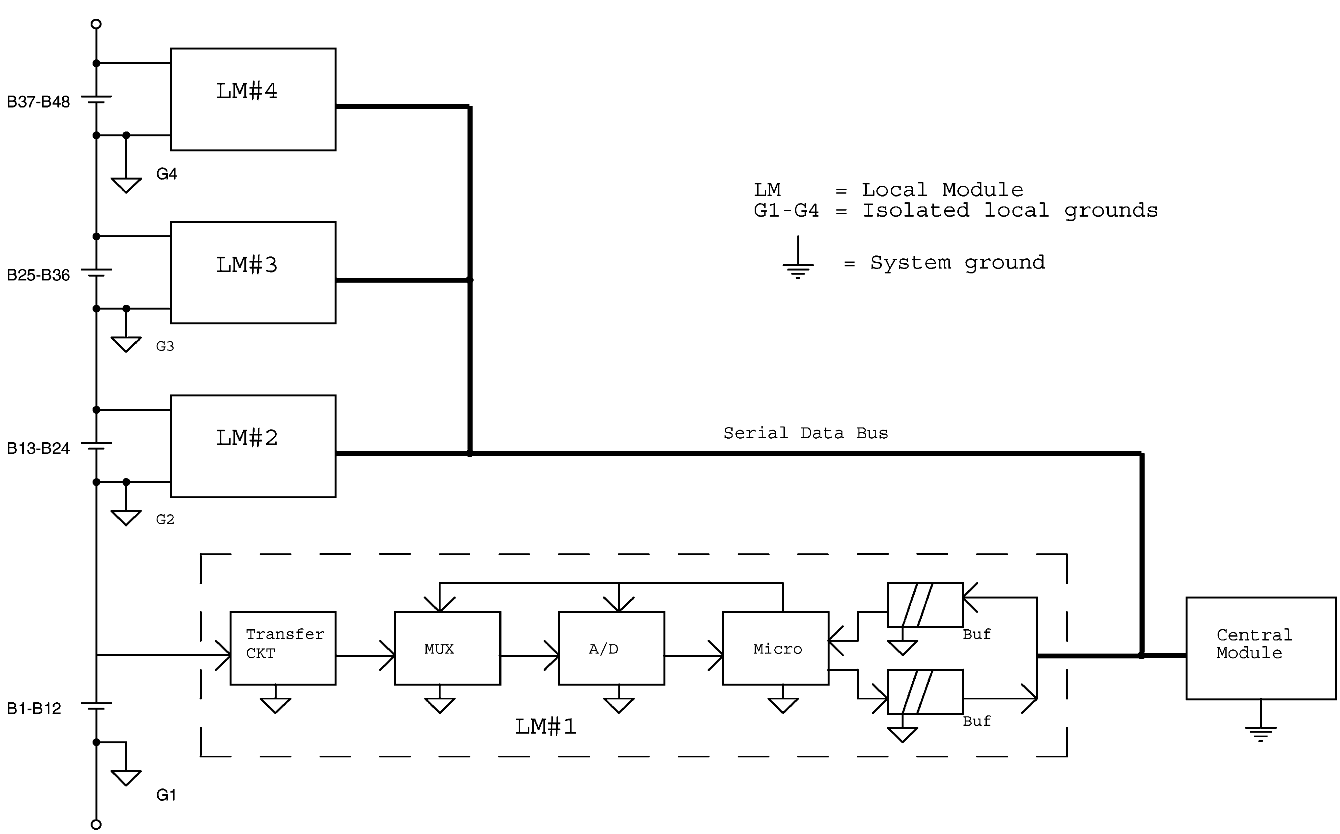

Fig. 2. Modularized battery management system.

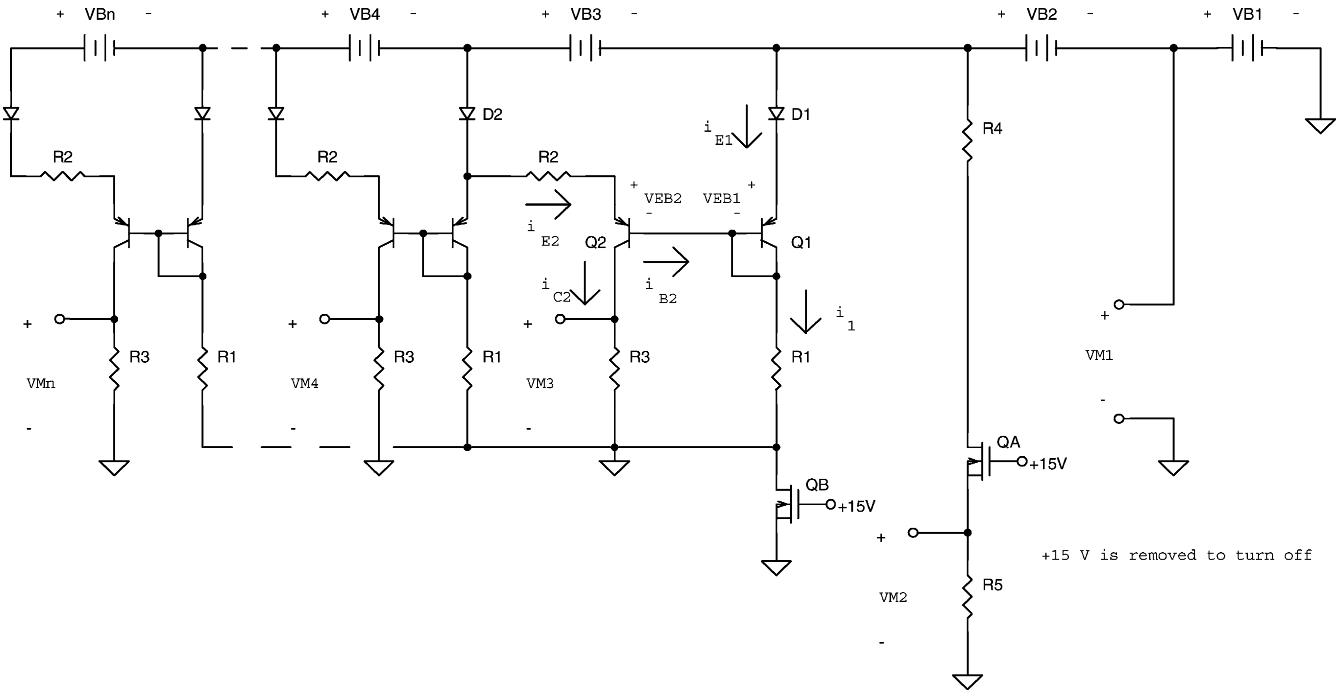

Fig. 3. Transfer circuit with discrete transistors.

this circuit has certain advantages over other methods, but it does require the matching of several discrete components, as discussed in [13]. The bipolar transistor circuits are inactive until Q_B is turned on, which provides a path for i_{E1} and i_{B2}. If V_{EB1} cancels V_{EB2} and V_{D1} cancels V_{D2} (R_1 is selected such that $i_1 \approx i_{C2}$),

$$i_{E1} = \frac{V_B}{R_2} \tag{1}$$

and

$$V_M = i_{C2} R_3 \tag{2}$$

Since,

$$i_{E2} = i_{C2} + I_{B2} \tag{3}$$

and

$$i_{C2} = \beta_2 i_{B2} \tag{4}$$

where β_2 = gain of Q_2

$$\frac{V_B}{R_2} = \frac{V_{M3}}{R_3} + \frac{V_{M3}}{R_3 \beta_2} = \frac{V_2(\beta_2 + 1)}{R_3 \beta_2} \tag{5}$$

or

$$V_M = V_B \left(\frac{R_3}{R_2}\right)\left(\frac{\beta_2}{\beta_2 + 1}\right) \tag{6}$$

If β_2 is sufficiently large, e.g. $\beta_2 > 100$,

$$\frac{\beta_2}{\beta_2 + 1} \cong 1 \tag{7}$$

and

$$V_M = \frac{R_3}{R_2} V_B \tag{8}$$

The diodes in the D1 and D2 positions are required to prevent leakage current that results from the reverse avalanche of the base to emitter junctions of the Q_1 transistors while the circuit is off, but they can be eliminated if V_{Bmax} is less than the V_{EB1} breakdown voltage. However, this means a diode would have to be placed in series with each R_1 (except the one for V_{Bn}) to prevent breakdown and the resulting leakage caused by battery segments to the left. If V_{B1} is <5 V, it can be measured directly as shown with a standard A/D converter. For higher voltages, a resistive divider similar to that for V_{B2} can be used for V_{B1}. Q_A prevents leakage current in the off state and its saturated R_{dson} is negligible compared to R_4 and R_5. If each V_M is processed by a microcontroller, initial tolerances can be reduced considerably, by using a calibrated test fixture and storing a correction factor in flash memory for each V_M.

Although initial tolerance errors can be reduced to a very low-level, temperature induced variations prove to be more difficult. For example, [13] presents data showing how temperature variations may create β variations that affect the approximation in (7); β effects can be reduced by replacing Q_1 and Q_2 with Darlingtons, but this probably means almost twice the number of discrete transistors since the selection of small surface mount Darlingtons is very limited. Variations in component matching also may increase as more parts are added.

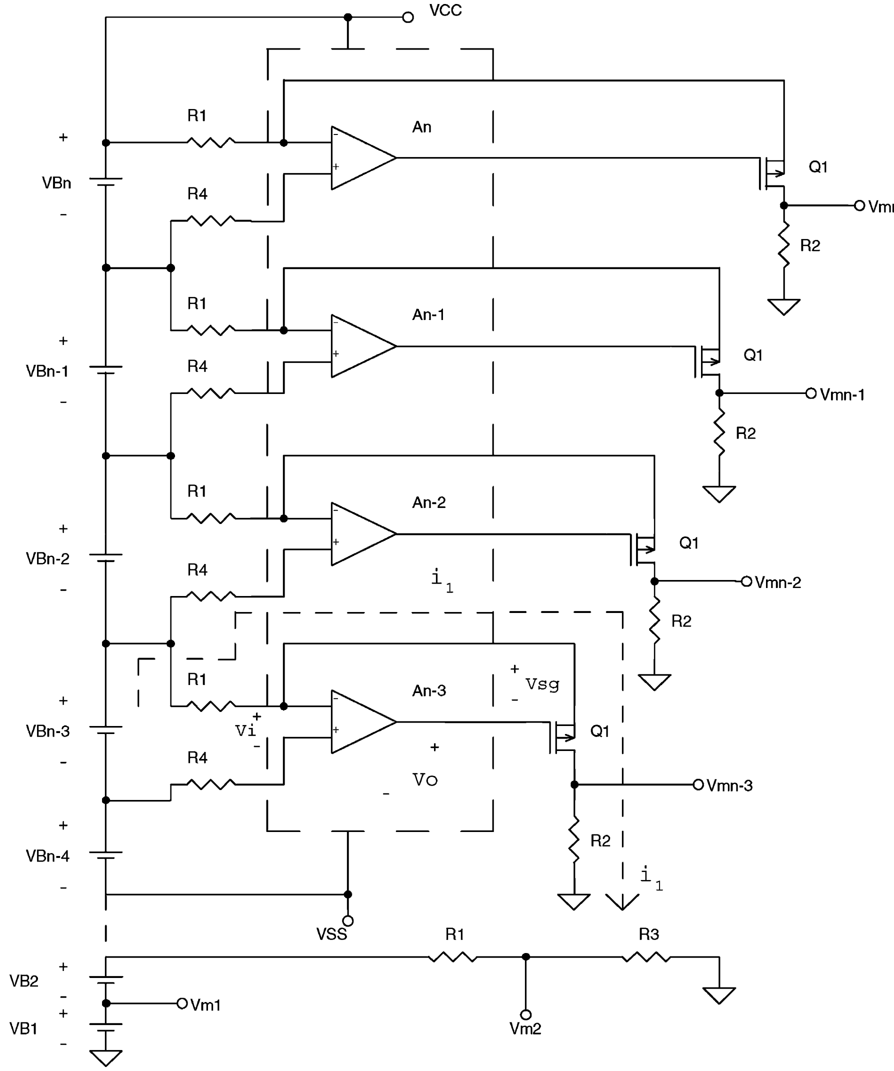

Fig. 4. Basic transfer circuit using Op Amps.

3. Op Amp transfer circuit

Fig. 4 shows another voltage transfer circuit that avoids the matching of discrete transistors required for Fig. 3. This particular design is intended for a pack with fairly low voltage segments, e.g., Li-ion cells which operate below 4 V dc. The battery pack serves as the power supply for the Op Amps and because of the low cell voltage, it is possible to use a low cost quad package, such as the LM224. Each of the measurement circuits for V_{B3} to V_{BM} is a simple amplifier based on a well-known transconductance amplifier found in references, such as [14].

Typical operation will be described for measuring V_{Bn-3}. If $i_1 = 0$, $V_i = V_{Bn-3}$, V_0 will be driven to almost 0 and $V_{SG} = V_{Bn-3} + V_{Bn-4}$. To achieve equilibrium, i_1 must reach a value such that

$$V_{Bn-3} = i_1 R_1 \qquad (9)$$

and

$$V_{Bn-4} = V_{SG} + V_0 \qquad (10)$$

V_0 will adjust so that V_{SG} maintains equilibrium, and

$$V_{Mn-3} = i_1 R_2 = \frac{R_2}{R_1} V_{Bn-3} \qquad (11)$$

This circuit avoids the β induced error of Fig. 3 and it is not necessary to use an Op Amp with an especially low input voltage offset drift. For example, even an inexpensive device, such as the LM224 (typical offset drift of ± 7 μV/°C [14]) produces the following results for $\Delta T = 50$ °C.

$$\Delta V = \pm 7 \times 50 = \pm 0.35 \qquad (12)$$

This means that $i_1 R_1$ would have to change by -0.35 mV to compensate. For $V_{Bn-3} = 4$ V, this represents an error of only −.009%, whereas the ±2 bit error of a 10 bit A/D is ±.25% (±10 mV) using a 5 V dc reference [15]. This means temperature variation is primarily dependent only on the temperature induced error of the R_2/R_1 ratio. The calibration procedure to reduce the initial tolerance is the same as previously described for the circuit in Fig. 3.

Since V_{M1} <5 V, it can be measured directly with the A/D converters found in most microcontrollers. A simple resistive divider for V_{M2} and the value of V_{B1} can be used to obtain V_{B2}, and this should provide the about same accuracy as for the other segments.

The basic circuit in Fig. 4 works quite well while the circuit is active, but it must be revised to avoid certain problems while it is off. These revisions are included in Fig. 5. The first of these problems is leakage current drawn from the battery pack while the circuit is supposed to be off. The supply current drawn by the Op Amps is typically small in comparison to the battery ratings, e.g., the specified maximum value for the LM224 is 3 madc [14]. However, even this low value can add up to a significant loss if the system remains in storage for several weeks, e.g., for a 6 Ah pack on a hybrid electric vehicle. Therefore, an optically coupled switch, S1, is used to disconnect from the pack when the 15 V on–off voltage is removed. However, in spite of S1, the Op Amp inputs remain connected to the pack and without further changes, some leakage current can still flow via these input lines. To open these paths, it is necessary to disconnect Vss using S2 and also disconnect the outputs using the Q_2 transistors. As explained earlier, since the R_{dson} of Q_2 is very small compared to R_1 and R_2, it does not affect the measurement accuracy. The gate voltage of 15 V dc $- V_M$ is adequate to saturate Q_2.

Although, these changes eliminate the leakage, the value of V_{SG} in the off state is variable and can drift above the breakdown value of Q_1. Therefore, the D1 zeners are added to protect these gates. Naturally, the Q_1 breakdown problem can be avoided by replacing the Q_1 FETs with BJT2 as in Fig. 6. However, in the off state, the forward biased emitter base junction of Q_1 provides a leakage path through R_1, back

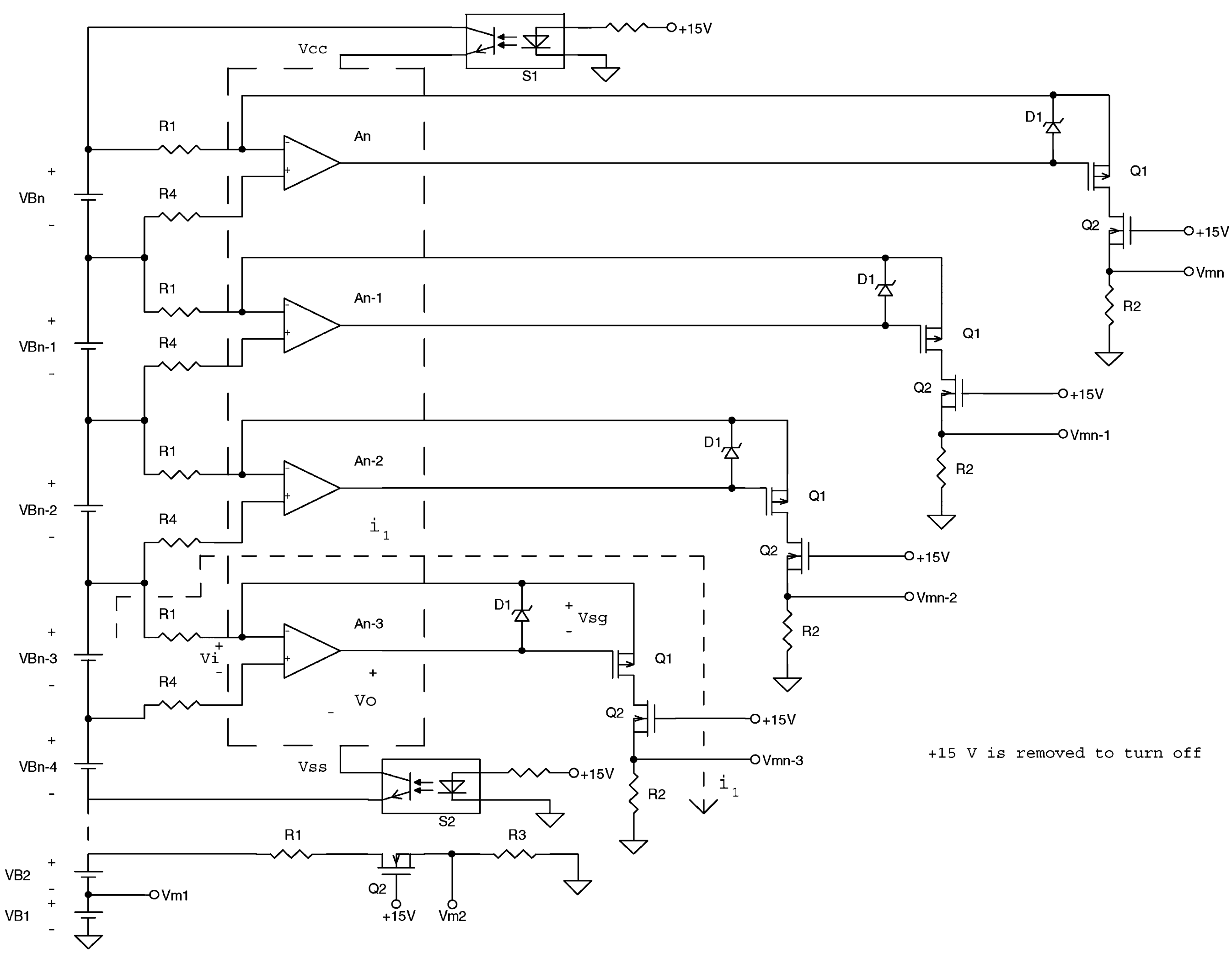

Fig. 5. Transfer circuit with revisions to avoid leakage and gate breakdown.

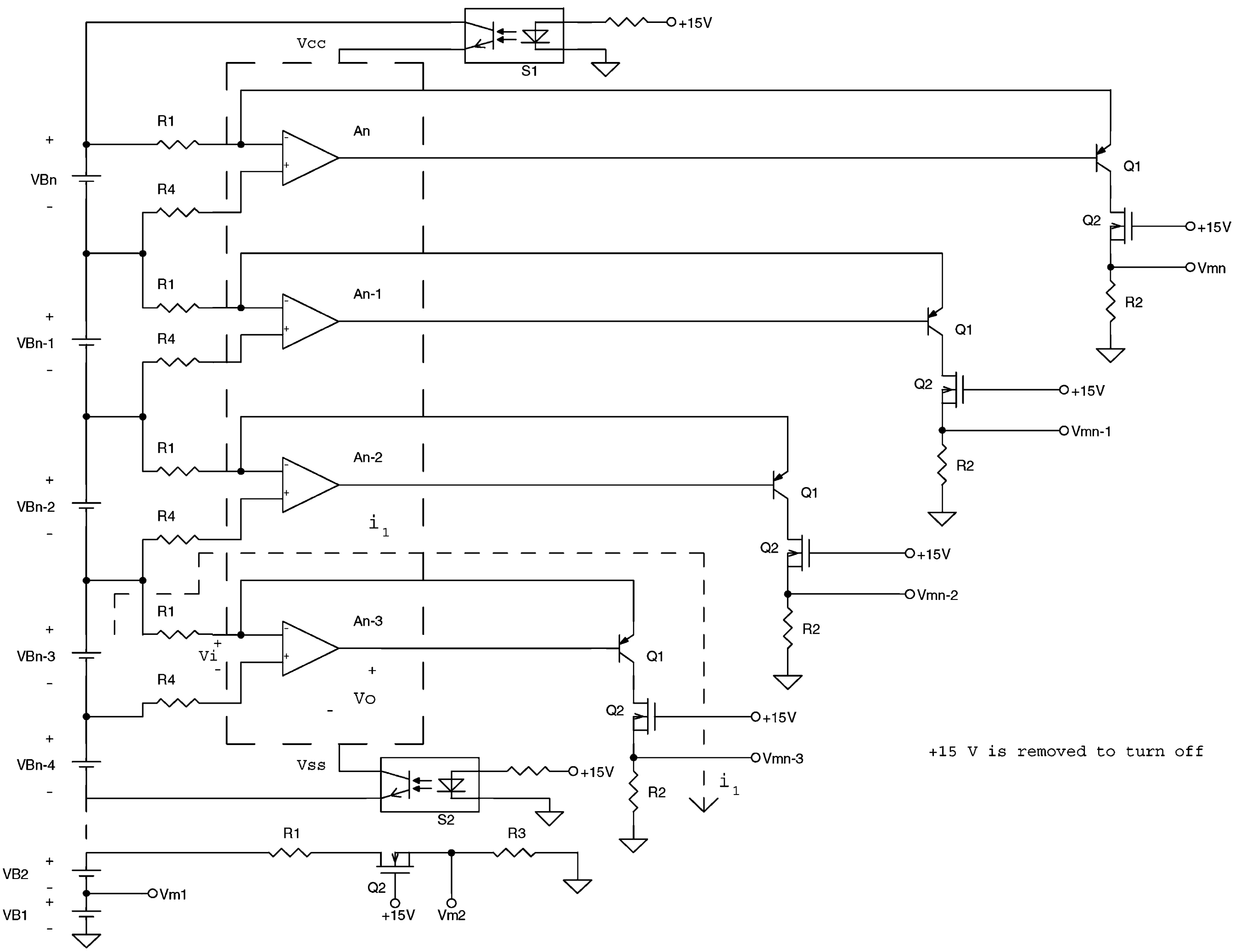

Fig. 6. Transfer circuit using BJTs for Q_1 transistors.

through the output of the Op Amp and eventually out of the Op Amp (+) terminal to R_4. Since this leakage presents a problem for long term storage, it is preferable to avoid it by using a FET for Q_1.

4. Experimental results

Fig. 7 shows a test circuit for comparing the temperature induced errors of the two transfer circuits. The components to the left of V_1 comprise the discrete circuit from Fig. 3, while those to the right are for the more recent Op Amp version in Fig. 5. The S_1, S_2 and Q_2 components in Fig. 5 were omitted for these experiments since leakage current in the off state was not an issue.

Two transistors from an MPQ7093 quad pack were used to minimize the V_{EB} variations between Q_1 and Q_2; R_5 was selected so Q_2 would have about the same I_E as Q_1 when $V_1 \cong 4$ V dc. A thick film molded resistor network was used to implement R_1–R_4 to minimize variations in the R_2/R_1 and R_4/R_3 ratios. Initial tolerances were ignored in these tests since the system can be calibrated initially using correction factors stored in flash memory as described earlier. The +12 V dc source is used only to provide an adequate power source for both circuits and its exact value is not critical. V_1 is the simulated battery voltage and has a maximum value of 5 V dc, which will also be the maximum value of V_{M1} and V_{M2}. This is consistent with Li-ion requirements which usually have a limit of about 4 V dc or less.

These tests used a DVM with a display resolution of four digits and the circuit was allowed to "soak" for about 15 min at each temperature setting. All components in Fig. 7 were located in the temperature chamber except V_1 and V_2.

Experimental results for $V_1 = 4.082$ and 1.970 V dc are shown in Figs. 8 and 9. These two values slightly exceed the useable range of most Li-ion batteries and thus they provide data at both extremes of I_E. The ΔV_{M1} and ΔV_{M2} deviations versus temperature indicate that either circuit would be acceptable for many applications, but the Op Amp version

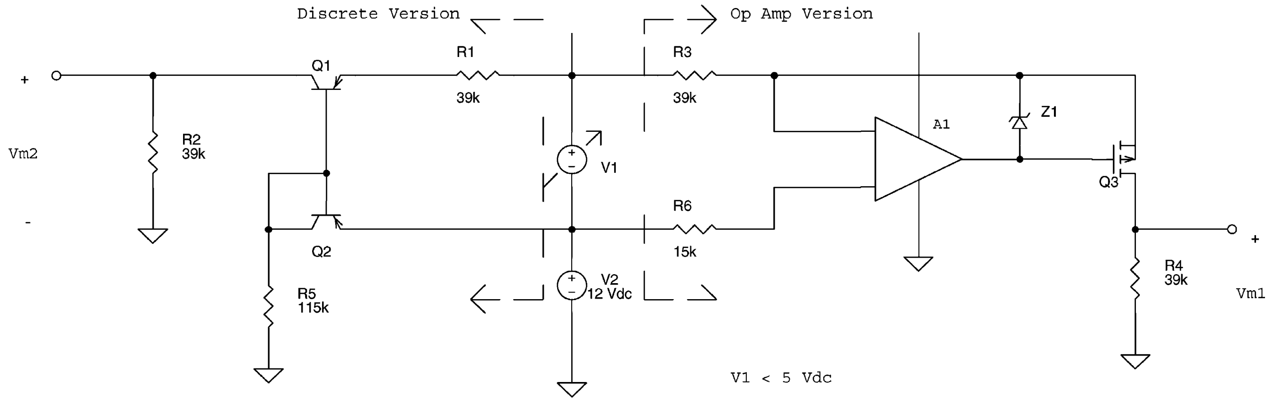

A1 : LM324
Q1, Q2 : MPQ7093 (4 PNPs/package)
Q3 : BSS84
Z1 : 12 V zener
R1-R4 : 39k +/- 2 % thick film molded resistor network,
+/- 100 ppm/oC

Fig. 7. Transfer test circuit.

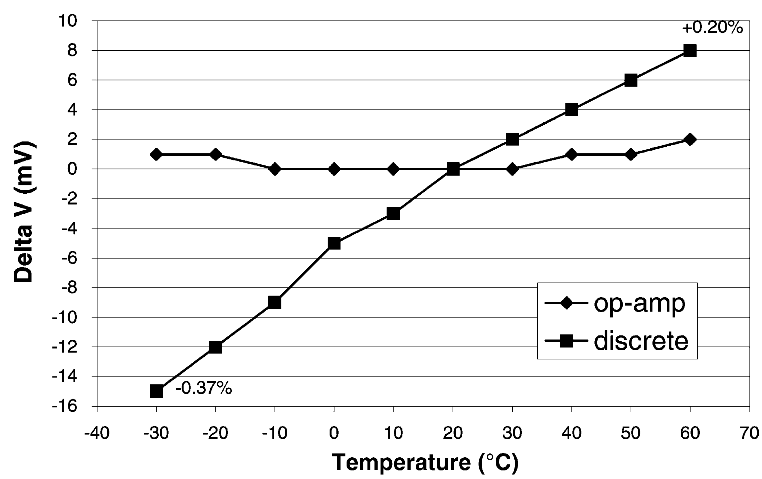

Delta V = (Vm) - (Vm @ 20 °C)

Fig. 8. Measured voltage vs. temperature for $V_1 = 4.082$ V dc in Fig. 7.

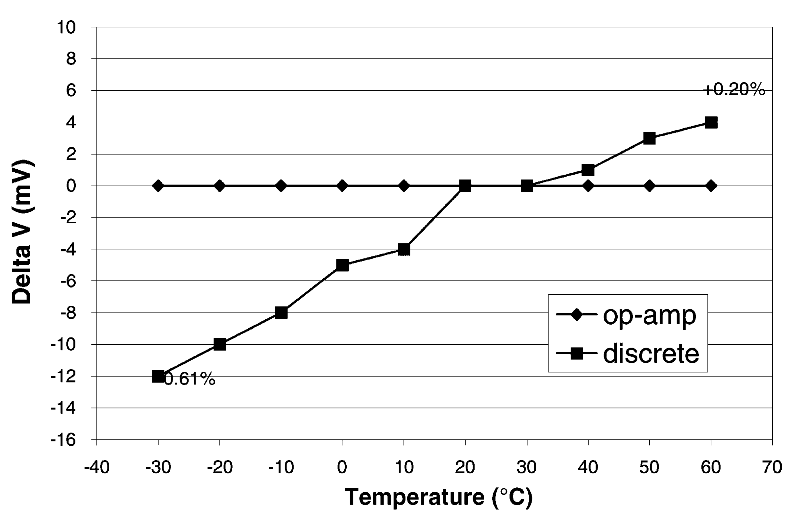

Delta V = (Vm) - (Vm @ 20 °C)

Fig. 9. Measured voltage error vs. temperature for $V_1 = 1.970$ V dc in Fig. 7.

has better accuracy because of the improved temperature compensation. The ΔV_{M1} data indicates the R_4/R_3 ratio remained almost constant for this resistor network and as predicted earlier, the typical offset voltage drift of $\pm 7\ \mu V/^{\circ}C$ for A1 apparently was not significant.

The ΔV_{M2} deviation for the discrete version is consistent with the expected β_2 variation in that β_2 increases with temperature. As shown by (6), V_{M2} also will tend to increase as β_2 increases with temperature. Apparently most the ΔV_{M2} variation is due to Q_1 and Q_2 since the ΔV_{M1} results imply that the variation in the resistance ratio is very minor.

5. Discussion

Although, the Op Amp version produced better results, either version will provide satisfactory performance for certain applications. Several types of batteries are currently under study for electric and hybrid electric vehicles, but most of the limited production cars presently use either lead acid, nickel metal hydride (NiMH) or lithium ion (Li-ion) batteries. The characteristics of each of these batteries are very different, and this implies different voltage measurement requirements.

Li-ion batteries will ignite if accidentally overcharged and this necessitates very accurate voltage measurements for each cell, such as those provided by the Op Amp version. Since the cell voltages are usually <4 V dc, low cost quad pack Op Amps can be used effectively to implement the circuit in Fig. 5. To measure V_{Bn-3} to V_{Bn} in Fig. 5, the supply voltage is connected between the top of V_{Bn} and the bottom of V_{Bn-4}, which provides a maximum value of about 20 V dc. This is well below the maximum limit of about 30 V dc for many common Op Amps.

Lead-acid and NiMH batteries also have maximum voltage limits that should be observed, but the issue here is a decrease in lifetime instead of an abrupt ignition. Therefore, monitoring of several cells together is usually adequate, such as the common practice of measuring a segment of six 2 V cells for lead-acid batteries. Since voltage accuracy is not as critical for these batteries as for Li-ion, the discrete component version is probably satisfactory, and it is also more compatible with the higher voltages that are present. The Op Amp version could be used for these batteries, but this may not be cost effective because of the supply voltage limits of most Op Amps. For example, some lead-acid batteries can reach about 16 V at full charge. To measure two batteries with two Op Amps in the same package, the Op Amp power source must connect across three batteries, which means a maximum voltage of 48 V dc. This is well above the maximum limit for most commercially available dual or quad pack Op Amps. Therefore, this application would require a single Op Amp for each battery and it would have a maximum supply voltage of 32 V dc since the power supply must be connected across two batteries. Since each Op Amp would now require its own S_1 and S_2 switches, the cost begins to escalate.

6. Summary

As predicted by analysis, experimental results show the Op Amp transfer circuit has better accuracy than the previous discrete component version. This is an important advantage for more critical applications, such as Li-ion batteries, where very precise voltage measurements are required over a wide temperature range. The circuit also should be economic for the low segment (i.e. each cell) voltages associated with Li-ion since low cost quad pack Op Amps can be used.

However, since the Op Amp circuit is always connected to the battery pack, provisions should be made to avoid certain leakage current paths within the Op Amps. This is easily done, but these extra components add significant cost to the circuit. As a result, for high voltage segments, such as those which are typical for lead-acid or NiMH packs, the previous discrete component version may be more cost effective.

Acknowledgements

This research was sponsored jointly by the US Department of Energy National Renewable Energy Laboratory and DaimlerChrysler, AG under Subcontract No. ACI-9-29118-01.

References

[1] D. Linden, Handbook of Batteries and Fuel Cells, McGraw-Hill, New York, 1984.

[2] Technical Marketing Staff of Gates Energy Products Inc., 1992.

[3] D. Berndt, Maintenance-Free Batteries, 2nd Edition, Research Studies Press Ltd., Somerset, UK, 1997.

[4] S.T. Hung, D.C. Hopkings, C.R. Mosling, Extension of battery life via charge equalization control, IEEE Trans. Ind. Electron. 40 (1) (1993) 96–104.

[5] Retzlaff W., Process and apparatus for charging a multi-cell battery, US Patent 5,438,250, 1 August 1995.

[6] T. Gottwald, Evaluation of battery charging with equalization, MSEE thesis, University of Toledo, OH, June, 1996.

[7] C. Pascual, P.T. Krein, Switched capacitor system for automatic series battery equalization, in: Proceedings of the Conference on IEEE Applied Power Electronics, February 1997, pp. 848–854.

[8] R. Park, Method of equalizing the voltages of individual cells of storage batteries, US Patent 4,331,991, 25 May 1982.

[9] N.H. Kutkut, H.L.N. Wiegman, D.M. Divan, D.W. Novotny, Charge equalization for an electric vehicle battery system, in: Proceedings of the IEEE Transactions on Aerospace and Electronic Systems, January 1998, pp. 235–246.

[10] N.H. Kutkut, H. Wiegman, D.M. Divan, D.W. Novotny, Design considerations for charge equalization for an electric vehicle battery system, in: Proceedings of the IEEE 1995 APEC, 1995, pp. 96–103.

[11] T. Gottwald, Z. Ye, T. Stuart, Equalization of EV and HEV batteries with a ramp converter, IEEE Trans. Aerospace Electron. Syst. 33 (1) (1997) 307–312.

[12] T. Gottwald, Z. Ye, T. Stuart, A High Frequency Electronic Equalizer for EV and HEV Batteries, in: Proceedings of the SAE Future Transportation Technology Conference, San Diago, CA, August 1997.

[13] D. Garrett, T. Stuart, Transfer circuit for measuring battery voltages in series packs, in: Proceedings of the IEEE Transactions on Aerospace and Electronic Systems, Vol. 33, 2000, p. 1.

[14] Linear Databook, National Semiconductor Corp., Santa Clara, CA, USA, 1982.

[15] Microcomputer Components Users Manual 08.97, Siemens, AG, 1997.